



**A Brief User's Guide to Single-chain Nanoparticles**

Journal:	<i>Polymer Chemistry</i>
Manuscript ID:	PY-REV-09-2014-001217.R1
Article Type:	Review Article
Date Submitted by the Author:	16-Oct-2014
Complete List of Authors:	Lyon, Christopher; University of New Hampshire, Chemistry Prasher, Alka; University of New Hampshire, Chemistry Hanlon, Ashley; University of New Hampshire, Chemistry Tuten, Bryan; University of New Hampshire, Tooley, Christian; University of New Hampshire, Chemistry Frank, Peter; University of New Hampshire, Chemistry Berda, Erik; University of New Hampshire, Department of Chemistry and Materials Science Program

## A Brief User's Guide to Single-chain Nanoparticles

Christopher K. Lyon,<sup>a</sup> Alka Prasher,<sup>a</sup> Ashley M. Hanlon,<sup>a</sup> Bryan T. Tuten,<sup>b</sup> Christian A. Tooley,<sup>a</sup> Peter G. Frank<sup>a</sup> and Erik B. Berda<sup>a,b\*</sup>

*a. Department of Chemistry, University of New Hampshire, Durham, NH 03824*

*b. Materials Science Program, University of New Hampshire, Durham, NH 03824 Ph. 603 862 1762 Fax 603 862 4278 Email: [Erik.Berda@unh.edu](mailto:Erik.Berda@unh.edu)*

**Introduction.** Precisely defined linear polymers folded into functional nanostructures, capable of completing complex tasks, are ubiquitous in nature. In this light, an obvious yet unmet research goal becomes apparent: exploiting our understanding of biomolecules to mimic this behavior in the laboratory using recent advances in controlled polymerization chemistry and the well-known theories of modern polymer physics. Advances in this technology will have applications in catalysis,<sup>1-5</sup> sensors,<sup>6</sup> nanoreactors,<sup>7</sup> nanomedicine,<sup>8-11</sup> etc.

The utility of biomacromolecules is a result of their well-defined tertiary structure: a specific three-dimensional shape with precise placement of functionality on the surface of the structure or its interior. Tertiary structure is permitted by a pristine primary structure, a quality that is currently inaccessible in synthetic polymers. Recent advances in contemporary controlled polymerization chemistry allow the synthesis of multiblock polymers with narrow molecular weight distributions<sup>12</sup> or materials with controlled monomer sequences<sup>13, 14</sup> by step-growth and chain-growth methods. These techniques are an enormous step forward, but still result in microstructural heterogeneities or broad molecular weight distributions. In analogy to the globular three-dimensional structures of folded biomolecules, dendrimers have been considered as a means to imitate this behavior owing to their monodispersity and highly regular structures. However, their syntheses are traditionally arduous and often result in

prohibitively low yields coupled with the inability to precisely control the placement of chemistry at the interior or specific sites on the surface. Although recent strategies employing “click” chemistry have improved upon traditional methods,<sup>15</sup> this situation is markedly different from the precise architectural control observed in nature.<sup>16</sup>

In order to fabricate functional soft nanomaterials that more closely mimic folded biomolecules in structure and activity, the new paradigm in polymer synthesis involves manipulating single polymer chains.<sup>17</sup> Among the various techniques employed to these ends, one in particular has garnered increased attention recently: the collapse or folding of linear polymer chains into architecturally defined nanostructures (Fig. 1). This process is simple in principle.

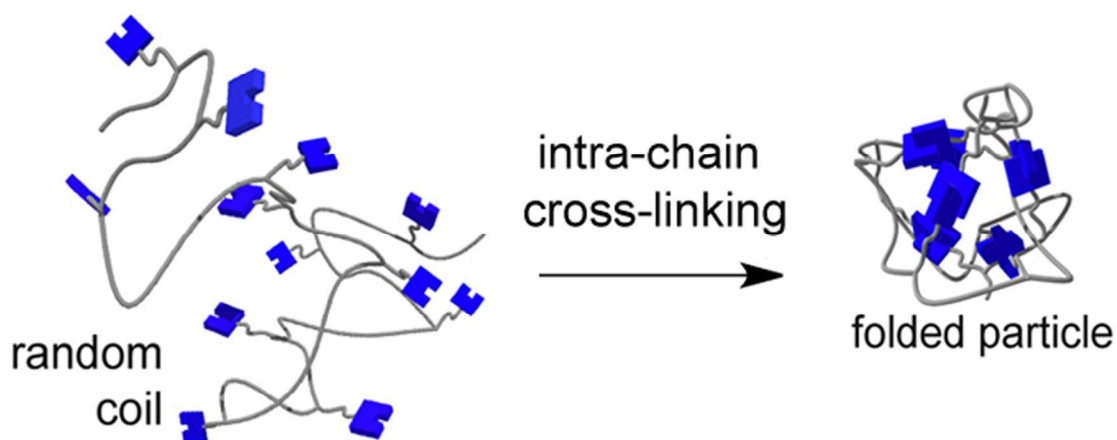


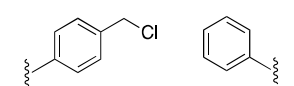
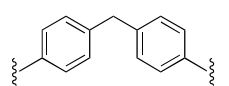
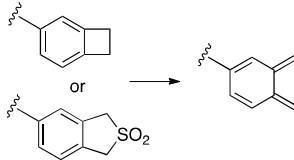
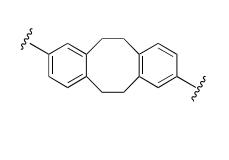
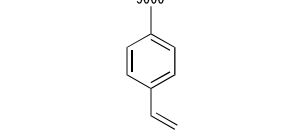
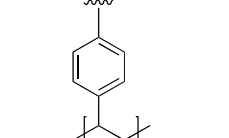
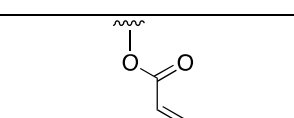
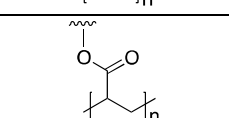
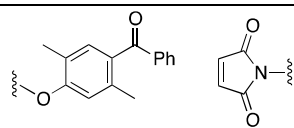
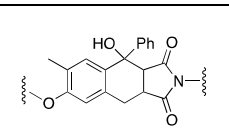
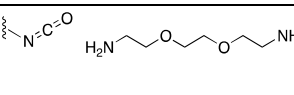
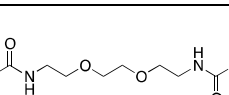
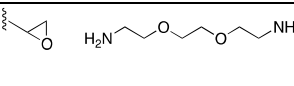
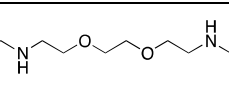
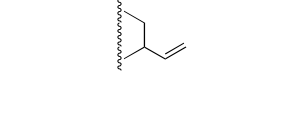
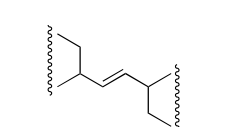
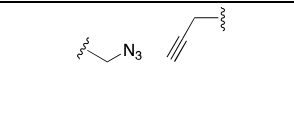
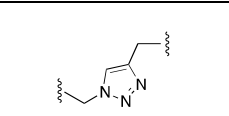
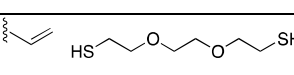
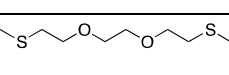
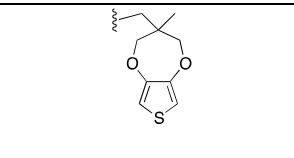
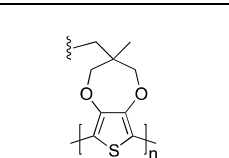
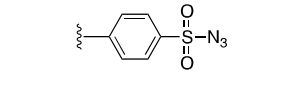
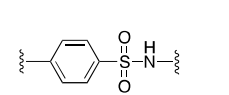
**Fig. 1** Linear polymer chains are decorated with functional groups that will promote intra-chain interactions when triggered in dilute solution. Reproduced from Ref. 18 with permission from Springer.

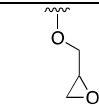
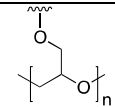
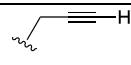
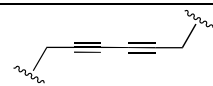
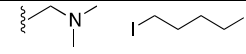
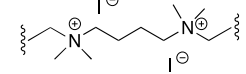
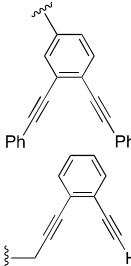
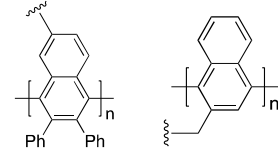
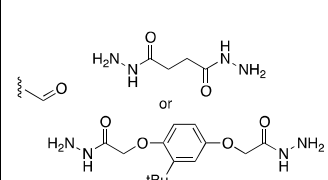
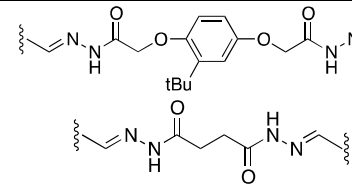
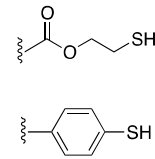
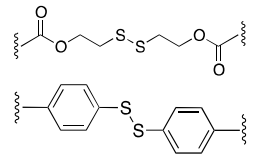
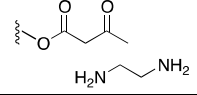
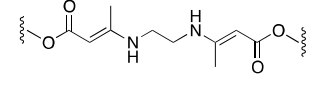
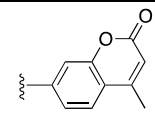
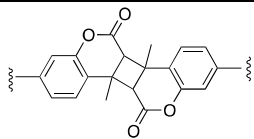
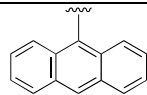
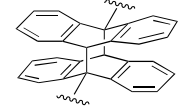
These single-chain nanoparticles (SCNP), while simple in concept, exhibit behaviors far more complex than initially anticipated and are currently the topic of intense focus by a number of research groups globally,<sup>19-22</sup> including our own.

Given that this is a rapidly growing area, we felt it would be useful to provide a kind of “user’s guide” to the SCNP literature. Rather than serve as an exhaustive review of every paper in the field, this document will highlight the current state of the art by examining (i) the chemistry and processing conditions used to synthesize SCNPs, (ii) the analytical techniques used to characterize SCNPs including a discussion of their behaviour and morphology, and (iii) current and potential applications. Our hope is that presenting the work in this way will serve as a handbook for current SCNP researchers, perhaps promoting collaboration, as well as a guide for those interested in entering this rapidly expanding field.

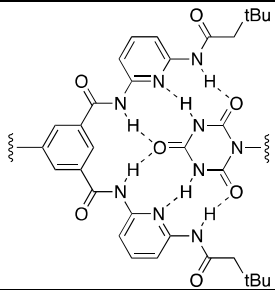
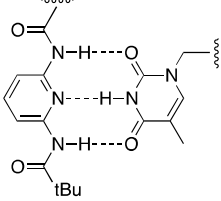
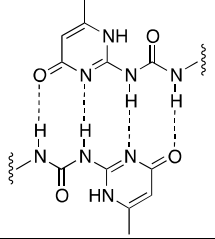
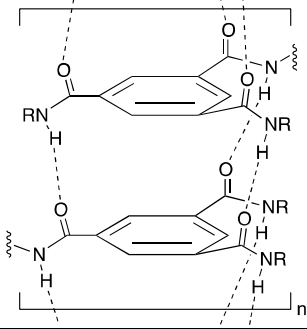
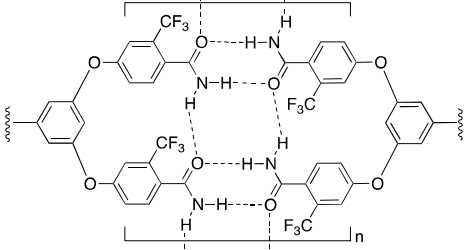
**I. Synthesis of SCNPs.** A variety of synthetic methodologies have been applied to the formation of SCNPs. In most cases, appropriately functional polymers are synthesized followed by post-polymerization transformation in dilute solution (typically < 1 mg/mL) to promote intra-chain cross-linking. Consequently, the chemical reactions that are used must meet the criteria of any effective post-polymerization functionalization reaction: they must be efficient and produce no side products.<sup>23</sup>

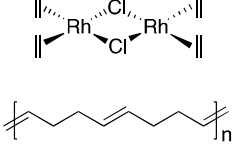
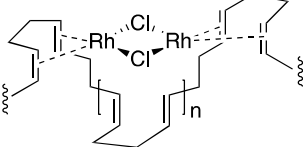
Nature takes advantage of many different orthogonal covalent cross-links (e.g. disulfides) and non-covalent interactions (e.g. hydrogen bonding, metal ligation), and dynamic covalent chemistry (e.g. acetal formation) in folded biomacromolecules. Taking this as inspiration, SCNP synthesis follows these same motifs. In this section we divide the discussion of intra-chain cross-linking chemistry into three major categories: covalent, dynamic covalent, and non-covalent. Table 1 highlights these three themes, along with illustrations of the chemical transformation used as well as the structure of the cross-link that is created by this chemistry.

Covalent chemistry			
Before cross-linking	Structure of cross-link	Type of chemistry	Ref
		Friedel-Crafts alkylation	24
		Thermal [4+4] cycloaddition	25-28
		Free radical polymerization	29, 30
			
		Photoinduced [4+2] cycloaddition	31
		Isocyanate-amine	32
		Epoxide-amine	
		Olefin metathesis	33
		Azide-alkyne "click" chemistry	8, 34-36
		Thiol-ene "click" chemistry	37
		Oxidative polymerization of thiophene	38
		Sulfonyl nitrene insertion/coupling	39

		Cationic polymerization of epoxide	1
		Glaser-Hay coupling	40
		Menschutkin reaction	41
		Bergman cyclization	42, 43
		Hydrazone formation	19, 44
		Disulfide formation	45, 46
		Enamine formation	47, 48
		Photodimerization of coumarin	7
		Photodimerization of anthracene	49

Non-covalent chemistry		
Structure		References

	<p>Hamilton wedge, cyanuric acid hydrogen bonding</p>	<p>50, 51</p>
	<p>Thymine, diaminopyridine hydrogen bonding</p>	<p>51, 52</p>
	<p>2-Ureido-4[1H]-pyrimidinone (UPy) hydrogen bonding</p>	<p>53-57</p>
	<p>Benzene-1,3,5-tricarboxamide (BTA) hydrogen bonding</p>	<p>2, 3, 6, 58, 59</p>
	<p>Dendritic self-complementary hydrogen bonding</p>	<p>60</p>

Metal coordination			
Before cross-linking	Structure of cross-link	Type of chemistry	Ref
		<p>Rhodium coordination</p>	<p>61</p>

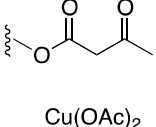
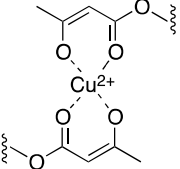
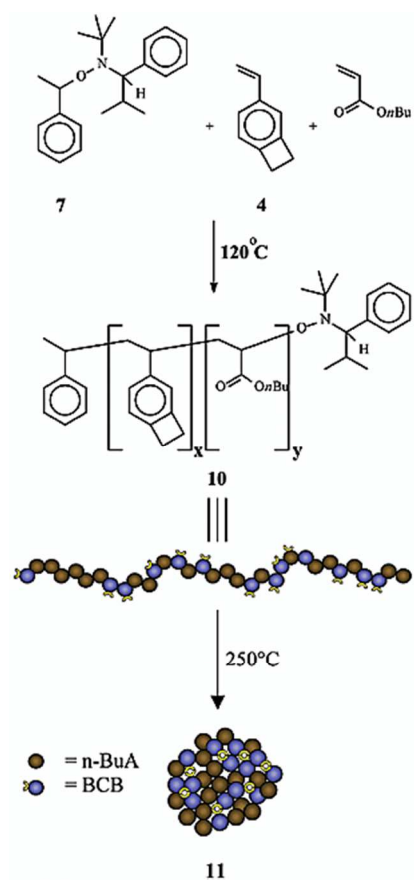
 <p style="text-align: center;">Cu(OAc)<sub>2</sub></p>		Copper coordination	5
--	---	---------------------	---

Table 1: Intra-chain cross-linking chemistry

**Covalent Cross-linking Reactions.** Hawker and coworkers synthesized architecturally defined SCNPs via intramolecular dimerization of the benzocyclobutene group at high temperatures (Fig 2).<sup>25</sup> As previously mentioned, SCNPs preparation requires low polymer concentrations (ca. 1 mg/mL) to avoid intermolecular coupling. The authors report syntheses of various random copolymers of 4-vinylbenzocyclobutene with various vinyl monomers via the nitroxide mediated free radical polymerization. A continuous addition method was employed in which a concentrated polymer solution was added to heated solvent, with an overall polymer concentration of ca. 2.5 mg/ml (0.05 M). The continuous addition technique proved to be much more efficient than typical ultra dilute conditions, by requiring less solvent while still preventing intermolecular coupling. The formation of nanoparticles using different polymeric backbones displays the versatility of this strategy. Subsequently, Harth and coworkers reported a more synthetically accessible vinylbenzosulfone (VBS) monomer, which exhibits similar crosslinking characteristics as the BCB derivatives.<sup>62</sup> The synthesis of this monomer is simpler, with mild reaction conditions and less purifications steps than previously reported methods. SCNPs were synthesized from VBS containing polymers using a continuous addition strategy, similar to the work involving the aforementioned BCB polymers.





**Fig. 2** Schematic representation of the intramolecular collapse of a linear polymer via BCB chemistry. Reprinted with permission from Ref. 25 Copyright 2002 American Chemical Society.

The high temperature conditions for these BCB reactions preclude the incorporation of sensitive functionalities in the polymer architecture. Harth and coworkers recently remediated this issue by placing an electron donating group on the cyclobutene ring, lowering the isomerization temperature to 150 °C. While the continuous addition strategy decreases the amount of solvent that is used, it is impractical to produce commercially relevant quantities of material by this method, a major challenge that is yet unmet in the SCNP community.

High efficiency, high functional group tolerance, and mild reaction conditions make “click” reactions an attractive candidate for synthesizing SCNPs.<sup>22</sup> To date, copper-mediated azide-alkyne cycloaddition,<sup>8, 34-36</sup> thiol-ene addition,<sup>37, 63</sup> and amine-isocyanate addition<sup>32</sup> click reactions have been used as cross-linking methods for SCNP fabrication. “Click” reactions involving alkynes and alkenes often involve protection or post-polymerization modification strategies, due to their incompatibility with radical polymerizations. Alternatively, the more sensitive reactive partner can be placed in an external crosslinking agent as not interfere with polymerization chemistry.

In interesting work by Pomposo and coworkers, direct polymerization of unprotected terminal alkynes was conducted via redox-initiated RAFT polymerization.<sup>40</sup> Subsequent exposure of a dilute polymer solution to copper-catalyzed Glaser-Hay coupling conditions led to SCNP formation.

O'Reilly and coworkers reported the synthesis of SCNPs via the tetrazine-norbornene reaction.<sup>64</sup> While not traditionally considered a “click” reaction, of this technique benefits from fast and quantitative conversion at room temperature with out the need for catalyst and therefore meets the “click” criteria at least in this context.

Photochemical reactions are often clean, high yielding, relatively fast, and require no chemical catalysts. A number of photoinduced coupling reactions have been examined for SCNP formation, including the photochemically triggered Diels-Alder reaction between 2,5-dimethylbenzophenone and maleimide,<sup>31</sup> the photo-dimerization of coumarin,<sup>7</sup> the photo-dimerization of anthracene,<sup>49</sup> and the photoinduced nitrile imine mediated tetrazole-ene cycloaddition.<sup>65</sup>

Zhu and coworkers reported photoinduced Bergman Cyclization to form polymeric nanoparticles via intramolecular collapse.<sup>42,43</sup> The desired reactive motif possessed high photoreactivity with phenyl substituted triple bonds and double bonds locked in a methylbenzoate ring. Various random copolymers containing enediyne monomer and butylacrylate were synthesized via SET-LRP. The resulting linear copolymers were further subjected to Bergman cyclization conditions in toluene under dilute conditions by the continuous addition technique to form corresponding nanoparticles.

The reactive sulfonyl nitrene moiety, formed by thermal extrusion of nitrogen from sulfonyl azide groups, has been used by Pu and coworkers to form SCNPs.<sup>39</sup> This reaction requires high temperature (190 °C), and the cross-links that are formed are not well-defined, due to the highly reactive nature of sulfonyl nitrenes. Similarly, Li and coworkers synthesized azido-functionalized polystyrene. The azido group forms a nitrene upon exposure to UV radiation and cross-links are formed by nitrene insertion. If the crosslinking is not driven to completion, it is possible to functionalize the remaining azide groups using click chemistry.

Coates and coworkers used olefin metathesis to synthesize polymer nanoparticles from linear polycarbonates containing pendant vinyl groups.<sup>33</sup> The copolymerization of vinylcyclohexene oxide, cyclohexene oxide, and CO<sub>2</sub> with a BDI-ligated zinc catalyst produced the desired vinyl-functionalized polymer. The degree of cross-linking mediated by Grubbs' catalyst can be easily monitored spectroscopically.

Thayumanavan and coworkers synthesized a copolymer of styrene, Fmoc protected aminostyrene, and chloromethylstyrene. The chloromethylstyrene was used as a

reactive handle to incorporate pendant styrene groups, which were subsequently polymerized in dilute solution using AIBN as an initiator, forming SCNPs. The Fmoc groups were then removed, resulting in amine-functionalized nanoparticles.<sup>29</sup>

Pomposo and coworkers recently reported the synthesis of SCNPs with catalytic activity.<sup>1</sup> Various linear polymer precursors with glycidyl functionality were collapsed via  $B(C_6F_5)_3$  catalyzed polymerization. Once the polymerization of the glycidyl units is complete, the catalyst remains in the nanoparticle. The authors found that linear polymers greater than 100 kDa required a higher degree of dilution in order to avoid intermolecular cross-linking. The catalytic activity of these nanoparticles is discussed further in the application section of this review.

Pyun and coworkers reported the synthesis of a novel propylenedioxy-thiophene functionalized polymer, which was cross-linked to synthesize SCNPs via oxidative polymerization of the thiophene units.<sup>38</sup> The ester linkage connecting the polystyrene backbone to the polythiophene was further cleaved to separate the polymer chains to prove the formation of polymerized propylenedioxy-thiophene side chains.

Zhao and coworkers reported the synthesis of SCNP shape amphiphiles, in which a hydrophobic polystyrene tail was attached to a hydrophilic poly(2-(dimethylamino)ethyl methacrylate)-based SCNP.<sup>41</sup> The p(DMAEMA) block was collapsed using a quaternization reaction of the tertiary amine with 1,4-diiodobutane. The authors also reported the solution behavior of the shape amphiphiles in polar and non-polar solvents. These shape amphiphiles represent SCNPs with multiple functionalities and well controlled three-dimensional structure.

**Dynamic Covalent Chemistry.** The synthesis of SCNPs via dynamic covalent bonds is an interesting route to adaptable and responsive nanostructures.<sup>66</sup> Under certain conditions, these bonds are reversible in nature and can be kinetically fixed or cleaved in response to change in environmental conditions, such as pH, oxidation, or temperature.

Fulton and coworkers utilized dynamic covalent acylhydrazone bonds to synthesize SCNPs with reversible character.<sup>19</sup> In this work, a bis(hydrazide) crosslinker was continuously added to aldehyde functionalized polystyrene, followed by catalytic trifluoroacetic acid (TFA). Before isolation, the TFA was quenched with triethylamine to kinetically trap the hydrazone bonds such that SCNPs would remain intact upon isolation. The cross-linking density of the nanoparticles was controlled by the amount of cross-linker added. Interestingly, no collapse was observed at higher cross-linking densities in these studies. The dynamic nature of the acylhydrazone bond was confirmed by formation of SCNPs via an exchange reaction of bis(hydrazide) crosslinker with copolymers adorned with monohydrazide. In a subsequent publication, Fulton et al reported a similar system, functionalized with oligo(ethylene glycol) side chains to impart thermoresponsive behavior. At low pH, a solution of nanoparticles is kinetically trapped; however, upon exposure to acid and heat, the thermoresponsive nanoparticles precipitate, followed by hydrogel formation. Upon cooling, this process is reversed.<sup>67</sup>

Pomposo, Fulton, and coworkers synthesized SCNPs capable of reversibly undergoing a coil to globule transition via enamine bond formation, which is reversible under acidic conditions.<sup>47</sup> Beta-keto ester functionalized linear polymers were synthesized and condensed with butylamine. SCNPs were synthesized by an enamine exchange reaction with ethylene diamine under dilute conditions. The cross-links were

cleaved upon addition of phosphoric acid and reformed again with additional ethylene diamine, exemplifying the reversible nature of the process.

Disulfides are a dynamic moiety of interest due to their presence in biological systems and sensitivity to redox chemistry. Work in this area from our laboratory involved the synthesis of anhydride functionalized linear polymers where by intramolecular disulfide linkages were installed by addition of 4-aminophenyl disulfide. The disulfides were reversibly cleaved and reformed in dilute solution by treatment with dithiothreitol (reducing) and iron (III) chloride (oxidative), respectively.<sup>45</sup>

**Non-covalent Chemistry.** Supramolecular interactions, such as H-bonding and  $\pi$ - $\pi$  interactions, are the dominant intra-chain linkage in folded biopolymers. Many groups have examined similar chemistry in SCNP synthesis. Often, monomers are functionalized with hydrogen bonding units that are protected in some way to prevent the polymers from forming aggregates during their synthesis. This is demonstrated in several publications by Meijer and coworkers involving 2-uriedopyrimidinone (UPy) dimerization (Fig 3).<sup>53-56</sup> Deprotection in dilute solutions allows the formation of intra-chain quadruple hydrogen bonds which in turn facilitates chain folding. The authors refer to these SCNPs as “metastable” because when cast into a film, the polymers remain soluble in chloroform; however, upon heating, the SCNPs uncoil and the UPy moieties form inter-chain linkages resulting in an insoluble supramolecular network.<sup>31</sup>

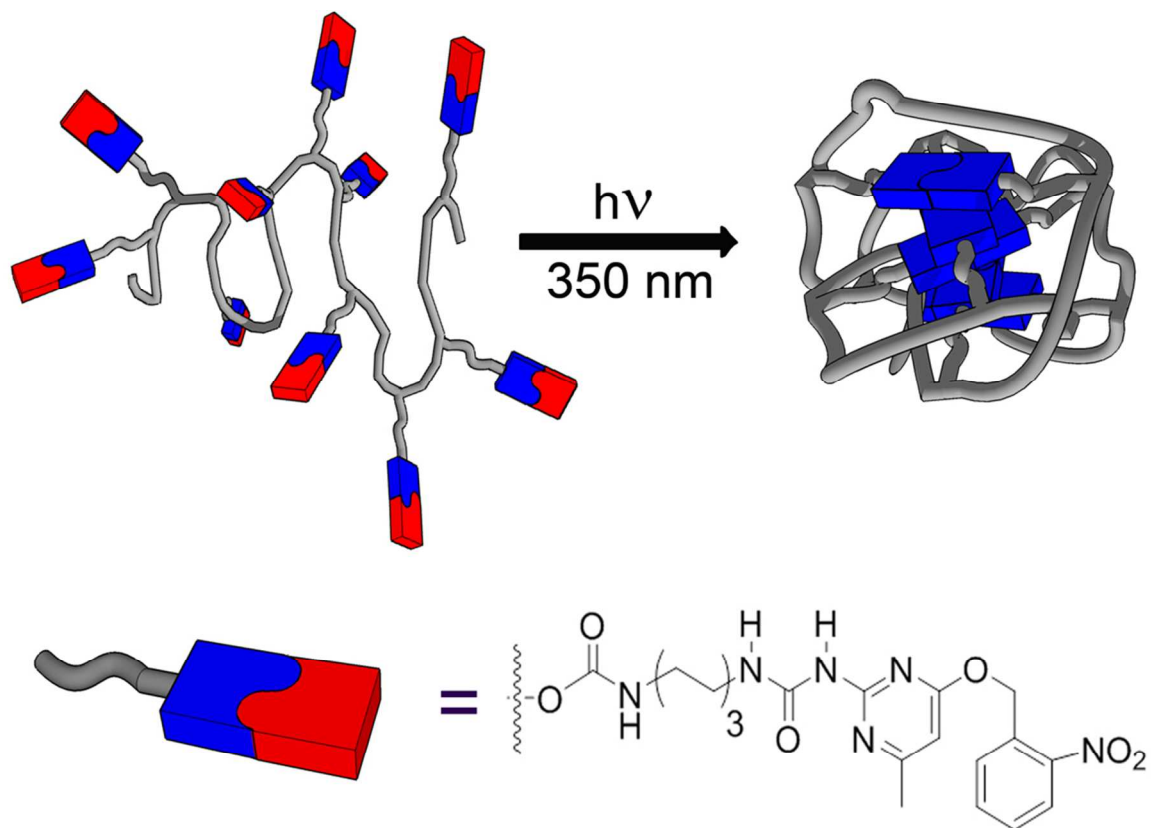


**Fig. 3** Schematic of SCNP formation via photo-deprotection of UPy groups. Reprinted with permission from Ref. 54 Copyright 2010 American Chemical Society.

UPy dimerization has been used to study the effect of several variables in SCNP formation. The rigidity of the polymer backbone, the placement of additional hydrogen bonding sites in the UPy linker, and the molecular weight of the polymer were shown to have little effect on the ability of a polymer to form supramolecular SCNPs, while solvent played an important role in disrupting or facilitating H-bond formation.<sup>57</sup>

Benzene-1,3,5-tricarboxamide (BTA) has been exploited in the field of supramolecular chemistry for its ability to form helical assemblies via hydrogen bonding;<sup>68</sup> consequently, it has also found use in SCNP synthesis. In one instance, a photoprotected BTA containing monomer is used to prevent aggregation during polymer synthesis.<sup>58</sup> In subsequent publications, this protection strategy was not necessary; BTA

containing monomers were simply polymerized directly in a solvent capable of disrupting H-bonds.<sup>2-4, 6, 69</sup> Alternatively, the BTA unit can be attached to a polymer via azide-alkyne “click” chemistry.<sup>56</sup>

Cucurbit[n]urils are known to form host-guest complexes with various aromatic molecules without necessitating the use of protection chemistry. In work by Scherman et al, methyl viologen and naphthyl functionalized polymers were combined with cucurbit[n]urils in dilute solution to form ternary host-guest complexes, resulting in SCNPs. In all cases, the polymers had to be studied at very low concentrations; above 0.1 mg/mL, significant aggregation was observed.<sup>70, 71</sup>

To date, there are only a few instances of using metal coordination to form intramolecular cross-links in SCNPs. The routes to these SCNPs have been relatively simple; a metal complex is introduced to a ligand-bearing polymer in dilute solution and a ligand exchange reaction occurs; the high local concentration of polymer-bound ligand drives SCNP formation forward. In one example, rhodium was bound by polycyclooctadiene, which contains 1,5-dienes.<sup>61</sup> Another example involves acac functionalized polymers containing copper (II) as a bridging metal for catalytic purposes.<sup>5</sup>

**Multiple Intra-chain Interactions.** It has been determined computationally<sup>72</sup> as well as with experiment that using multiple orthogonal intramolecular interactions results in more compact globular SCNPs. Hosono et al combined UPy and BTA units in a block copolymer to form SCNPs with orthogonal hydrogen bonding dimers (Fig 4).<sup>56</sup> Additionally, Altintas et al reported a polymer folded by two different orthogonal hydrogen bonding dimers.<sup>51</sup> Another example by Chao et al involved ROMP-synthesized



polyolefins collapsed via the supramolecular association of pendant tetraaniline units and covalently crosslinked by thiol-ene “click” chemistry involving the olefins in the polymer backbone.<sup>63</sup>

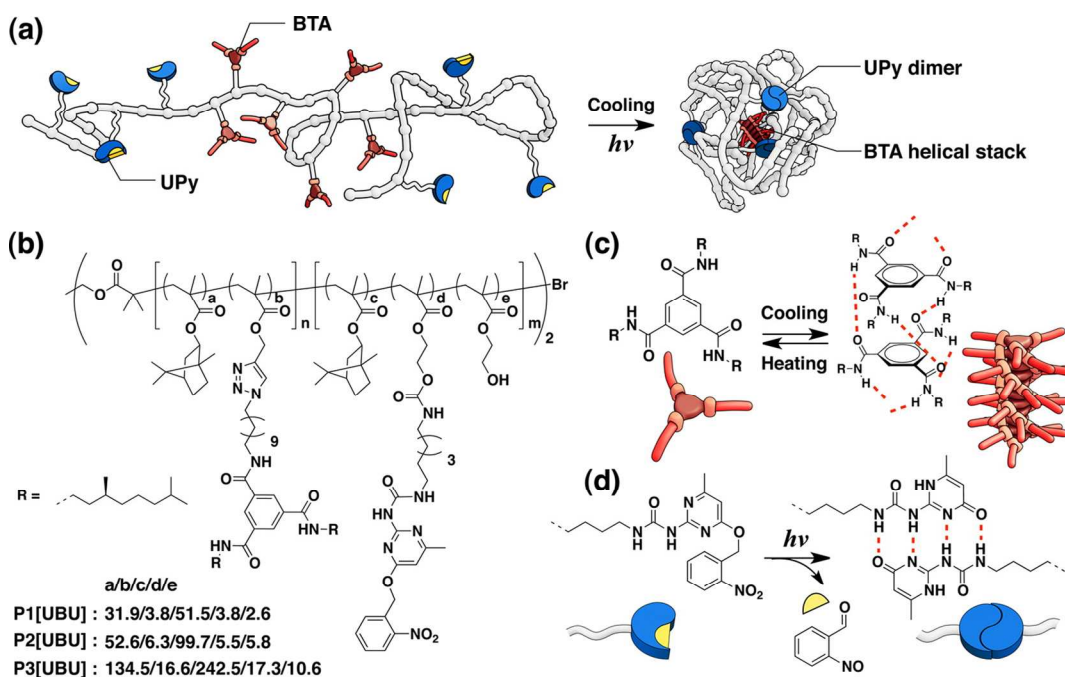


**Fig. 4** Design of a triblock copolymer bearing BTA and UPy moieties. (a) Graphic representation of SCNP formation; (b) Chemical structure of triblock copolymers; (c) helical self-assembly of chiral BTAs via threefold-symmetric hydrogen bonding; (d) photoinduced dimerization of *o*-nitrobenzyl protected UPys via quadruple hydrogen bonding. Reprinted with permission from Ref. 56 Copyright 2012 American Chemical Society.

**Outlook.** Surveying the literature it becomes clear that SCNP synthesis using a singular covalent chemistry as an intra-chain cross-link, and even the use of dynamic covalent chemistry or various supramolecular interactions is a well developed, proven technique. Moving this field forward will require innovations with relation to the use of multiple

intra-chain interactions, as only a few examples are present in the current literature. Exploring more complicated polymer architectures such as block copolymers and branched structures is an open area for innovation. Combining SCNP synthesis techniques with advanced polymer syntheses that control monomer sequence or functional group placement such as work by Perrier,<sup>12</sup> Lutz,<sup>14</sup> and Whittaker,<sup>73</sup> or well-defined step-growth chemistry such as ADMET,<sup>13</sup> provides possibilities that could take the current state of the art one step closer to the structural precision found in natural folded macromolecules.

**II. Characterization of SCNPs.** The corroboration of data provided by multiple techniques is often required to characterize SCNP formation. The appearance or disappearance of functional groups involved in the cross-linking chemistry and changes in the size and morphology of polymer structure can be detected using the techniques described in this section. Importantly, it is often necessary to use techniques that are sensitive enough to detect small concentrations of aggregates that may be formed by intermolecular cross-linking to prove the single molecule nature of these nanostructures.

**Size Exclusion Chromatography.** Size exclusion chromatography (SEC) has been an invaluable tool in understanding and characterizing SCNPs. Early papers began with qualitative SEC measurements based on standards<sup>24, 25</sup> and have since evolved into more quantitative measurements using multiple in-line detectors such as multi-angle light scattering (MALS) and viscometry.

Standalone SEC measurements are vital to understanding the behavior of SCNPs. While the molecular weight of globular SCNPs cannot be accurately measured using linear polymer standards, SEC provides other valuable data. An in depth study performed by Harth and coworkers provides an excellent example.<sup>25</sup> In this work random copolymers of styrene and vinylbenzocyclobutane (BCB) were used to create a family of SCNP. The molecular weight of these linear polymers was measured using SEC with polystyrene standards. Upon collapse, SEC measurements showed that all of their polymers had an increase in retention time and a decrease in apparent molecular weight. Since the BCB cross-linking does not produce any side products, the decrease in apparent molecular weight can be directly attributed to a decrease in hydrodynamic volume, which is principally what is measured by traditional SEC. Additionally, the authors used the change in apparent molecular weight to calculate the decrease in hydrodynamic volume. This data was corroborated by dynamic light scattering (DLS) measurements. <sup>1</sup>H NMR was also used to confirm the complete disappearance of the BCB moiety, confirming spectroscopically that changes in solution volume can be attributed to this chemistry.

Often, a decrease in polydispersity index ( $\mathfrak{D}$ ) is observed via SEC when a chain transitions from a linear coil to a SCNP. In a computational study,<sup>74</sup> Pomposo et al examined SCNP formation assuming theta conditions for all samples so that a SCNP can be treated as a small linear polymer with a comparable hydrodynamic volume. They found this decrease in polydispersity index arises from the standard SEC calibration equation ( $M_{app} = cM^\beta$ ), where the apparent molecular weight uses a scaling factor derived from a hydrodynamic radius equation. This research illustrates the merits in studying the complex physics of the intra-chain cross-linking of polymers via various mathematical

and computational methods. Full three-dimensional modeling of these materials is still needed in order to include a wider range of collapsing chemistries and represents an open area of research opportunity. Even though quantitative data cannot be collected directly from standalone SEC, it still provides an important tool in characterizing SCNPs. Specifically, it is used to observe a qualitative decrease in hydrodynamic radius, and also provides insight regarding intramolecular vs. intermolecular coupling.

**Light Scattering.** The principles of light scattering were established by prominent scientists such as Einstein,<sup>75</sup> Raman,<sup>76</sup> Debye,<sup>77</sup> and Zimm<sup>78</sup> at the beginning of the 20<sup>th</sup> century. It has since been the basis of one of the most useful forms of absolute characterization of macromolecular suspensions and solutions. Light scattering is an absolute method; the molar mass of large macromolecules is calculated based on first principles and consequently does not produce data relative to standards.<sup>79</sup> In regard to SCNPs, dynamic light scattering (DLS) and multi-angle light scattering (MALS) are both indispensable characterization techniques. Work from our laboratory has shown that using a MALS detector in-line with an SEC can prove that the molecular weight is consistent from parent polymer to SCNP.<sup>45, 49</sup> Several groups have also used DLS as a method for confirming this result.<sup>31, 37, 80</sup>

**Viscometry.** Another valuable technique in the characterization of SCNPs is solution viscometry. A particle's intrinsic viscosity is related to its molecular weight by the Mark-Houwink equation (equation 1). Using the intrinsic viscosity measurement gathered by the viscometer and the molar mass data from MALS, "K" and "a" coefficients can be calculated which relate to polymer conformation and the interaction between polymer

and solvent. Viscometry is also useful in calculating hydrodynamic volume ( $V_h$ ) which can further be used to calculate hydrodynamic radius ( $R_h$ ) via the Einstein-Simha Relation (equations 2 and 3).

$$\text{Equation 1: } [\eta] = KM^a$$

$$\text{Equation 2: } V_h = M[\eta]/(2.5 N_A)$$

$$\text{Equation 3: } R_h = (3V_h/4\pi)^{1/3}$$

$[\eta]$  is intrinsic viscosity,  $M$  is molar mass,  $V_h$  is hydrodynamic volume,  $N_a$  is the Avagadro constant, and  $R_h$  is hydrodynamic radius.

Hawker et al used viscometric measurements to characterize the formation of SCNPs synthesized using intra-chain isocyanate chemistry (Fig 5).<sup>32</sup> The intrinsic viscosity of a polymer decreases as the degree of intramolecular cross-linking increases. In this case the authors used two polymer samples: 100 kDa, 150 kDa, and their SCNP counterparts, which were formed using an external diamine cross-linker. As expected, the higher molecular weight linear polymer had greater intrinsic viscosity than the lower. However, for the SCNPs, despite a 50% increase in molecular weight compared to the parent polymers, the intrinsic viscosities of both samples decreased, and were similar to one another. This is consistent with the prediction made by Einstein; that the intrinsic viscosity of a constant density sphere is independent of its molecular weight, i.e.  $5/2$  divided by the sphere density.

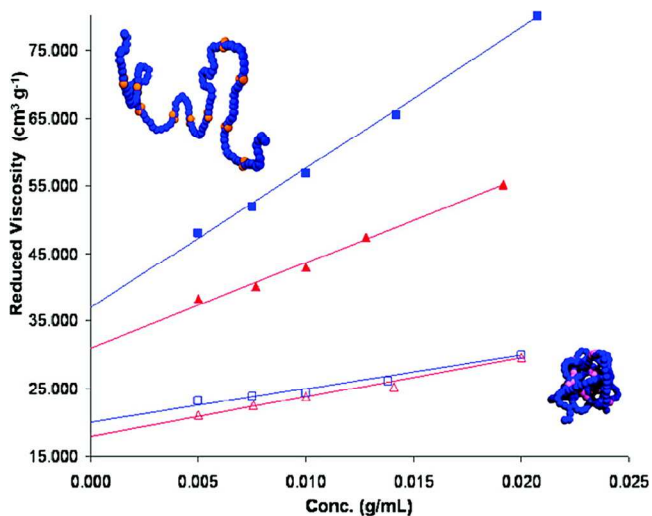


**Fig. 5** Plot of (a) reduced viscosity versus concentration for control copolymers (■, 150 kDa; ▲, 100 kDa) and (b) their analogous cross-linked nanoparticles (□, 150 kDa; △, 100 kDa) in THF. Reprinted with permission from Ref. 32 Copyright 2009 American Chemical Society.

**Nuclear Magnetic Resonance Spectroscopy (NMR).** The formation of cross-links in SCNPs has been confirmed by monitoring the appearance or disappearance of signals from external or internal cross-linkers in  $^1\text{H}$  NMR. Some laboratories have shown that other NMR techniques can be useful in observing the coil-to-SCNP transition. Zhao and coworkers observed SCNPs formed by the intramolecular photodimerization of coumarin using  $^1\text{H}$  NMR spin-spin relaxation time ( $T_2$ ).<sup>7</sup> Spin-spin relaxation time is altered by molecular motion. An increase in the degree of dimerization showed an increase in the spin-spin relaxation time, which confirms a dramatic increase in the fraction of chain segments having reduced mobility upon collapse. Relaxation time measurements were made at varying percentages of photodimerization, which indicated reduced mobility with increased degree of cross-linking. Reduction of polymer proton signals was also

observed in the spectra from random coil to globule. Loinaz and coworkers demonstrated the use of DOSY experiments to determine the diffusion coefficient of poly(N-isopropylacrylamide) based thermoresponsive SCNPs in solution, which is inversely proportional to the hydrodynamic volume. The intramolecular collapse lead to an increase in the diffusion coefficient, as further evidence of the formation of collapsed SCNPs.<sup>35</sup>

**Characterizing the Morphology of SCNPs.** One of the most challenging aspects of the characterization of SCNPs is accurately deciphering their morphology, which is highly dependent on solvent choice and concentration. A similar situation occurred in the characterization of dendrimers. As Meijer and coworkers discussed in a detailed review,<sup>16</sup> the initial expectation of dendrimer morphology was not exactly what was encountered through detailed characterization studies. As more studies are published, it is becoming apparent that the expected morphology of SCNPs is not always consistent with experimental results. Solution-free microscopy techniques, primarily atomic force microscopy (AFM) and transmission electron microscopy (TEM), have provided insight into the size, shape, and aggregation of SCNPs. Characterization of SCNP solution morphology has also been achieved using small-angle neutron scattering (SANS) and small-angle X-ray scattering (SAXS). Currently a combination of microscopy and scattering techniques along with molecular simulations can give insight into the true nature of SCNPs. To observe individual SCNPs, low concentration solutions (typically around 0.01 mg/mL) have been used, while higher concentrations have shown the formation of aggregations. Certain trends are observed across several studies. As

expected, an increase in molecular weight of the parent polymer chains results in an increase in particle size, while an increase in cross-linking decreases the particle size.

Detailed AFM studies were carried out by Meijer and coworkers.<sup>54-53</sup> Multiple polymer chains decorated with 2-ureido-pyrimidonone (UPy) units protected with a photocleavable *o*-nitro-benzyl group for UV induced quadruple hydrogen bonding intramolecular collapse were synthesized. The authors were able to deduce the possible morphology of SCNPs formed from different polymer chains using AFM. Considering the adsorbed particles to be hemi-ellipsoidal, a calculation for the diameter of the particles was developed. Samples of these SCNPs at dilute concentrations show AFM images of individual SCNPs with a size distribution similar to GPC results (Fig 6). At higher concentrations, aggregation occurred, forming a variety of unique arrays based on solvent and concentration choice.

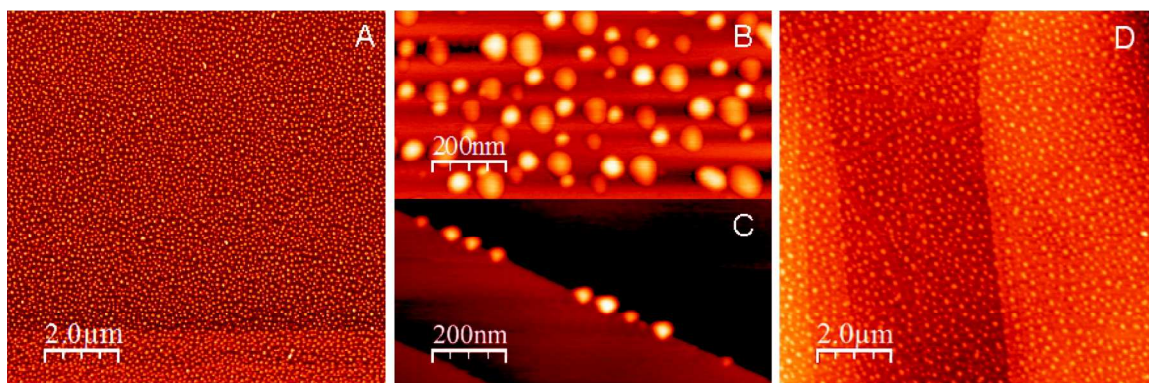


**Fig. 6** AFM images of single-chain nanoparticles. Panels A and B are on mica, while panels C and D are on graphite. Reprinted with permission from Ref. 53 Copyright 2009 American Chemical Society.



In another study, Meijer and coworkers were able to monitor the deprotection of UPy groups to induce chain collapse by AFM.<sup>54</sup> Sample concentration and choice of surface and solvent strongly affected these data. Furthermore, a difference between aggregates and individual particles was determined to ensure the characterization applied truly to SCNP and not multi-chain aggregates. In this study this difference was evident in height and phase images in which SCNPs showed a darkened core in contrast to no observed changes in phase for multi-chain aggregates.

AFM sample preparation involves drop casting onto substrates, which can induce particles to concentrate in the center of a droplet during the final stages of evaporation, causing aggregation. Meijer and coworkers studied this particle aggregation mediated by solvent evaporation.<sup>55</sup> To contrast individual SCNPs versus aggregation they conducted AFM experiments designed to intentionally induce particle aggregation. The evaporation rate was altered by changing the vapor pressure and solvent surrounding the substrate surface. Slow evaporation resulted in an increase in aggregation. The authors concluded that the major factors dictating morphologies observed by AFM are nanoparticle mobility before solvent evaporation and the amount of time required for solvent evaporation.

When SCNPs are drop cast onto a level surface, the morphology of the nanoparticle is altered upon drying; this morphology change has been observed in both AFM and TEM studies. AFM allows for the dimensional analysis of SCNPs, but TEM results have had better diameter correlation with DLS data than AFM, most likely due to the error resulting from the broadness of the AFM tip. In a study by Zhao and coworkers, a direct comparison of AFM, TEM, and DLS results for multiple nanoparticles revealed that AFM indicated rather large diameters while TEM results were much closer to the

DLS determined hydrodynamic diameter.<sup>41</sup> Similar results were obtained by Pomposo et al in a recent publication.<sup>1</sup> These studies indicate that TEM provides a more accurate image of the diameter of SCNPs as they behave in solution, although the diameter is still underestimated as they are swollen in solution and more compact once dry. Direct comparison of results from varying techniques may differ not just from instrumental effects but also due to sample preparation. Although correlations can be made, the profound effect of solvent choice and concentration on SCNPs morphology makes comparison of results from different sample preparation across different techniques difficult. It becomes important, in light of this knowledge, to use multiple methods of characterization and benchmark these data to the growing body of literature in this area.

While solvent free microscopy techniques provide valuable information on the morphology of SCNPs, their behavior in the absence of solvent and their interactions with substrates are still not entirely understood. For species that exist in solution, true morphology can only be observed with techniques that allow for characterization in solution. Small angle scattering techniques like small-angle neutron scattering (SANS) and small-angle X-ray scattering (SAXS) are becoming more common for the characterization of SCNPs. Both SAXS and SANS allow SCNPs to be directly characterized in solution.<sup>72</sup> TEM and AFM tend to display compact morphologies while SAXS and SANS results indicate less compact morphologies under good solvent conditions. These small angle scattering techniques have been used by many groups to measure the radius of gyration and observe form factors of SCNPs.<sup>1, 2, 9, 72, 81, 82</sup> Additionally, molecular dynamic (MD) simulations have proven useful in aiding researchers understand the data provided by small angle scattering techniques.<sup>72,9,1</sup>

Meijer and coworkers have demonstrated the use of SAXS to provide further evidence of SCNP formation in which a clear reduction in the radius of gyration from coil to globule results.<sup>81</sup> In a recent publication by O'Reilly and coworkers, large  $R_g$  values were obtained using SANS while AFM and TEM provided a more compact image with a smaller size predicted.<sup>64</sup> Increased SANS values were attributed to SCNP aggregations at room temperature, corroborated by DLS temperature studies. These results are an indication that data from solvent free techniques can be misrepresentative of how SCNPs behave in solution. Molecular dynamic simulations have shown that when decreasing the quality of solvent, increasingly compact conformations result, which is consistent with the compact morphologies that are constantly observed in solvent-free techniques.<sup>9</sup>

In studies by Pomposo et al a comparison of heterofunctionalized nanoparticles and their homofunctional counterparts was made both experimentally and using MD simulations based on generic bead-spring models.<sup>72</sup> Experimental SEC/MALS traces and SAXS data both showed more compact nanoparticles for heterofunctional species compared to their homofunctionalized counterparts, this was consistent with MD simulations. Slightly larger sizes were observed in SAXS data in comparison to simulations but were attributed to bending and torsional barriers of the actual polymer that were not taken into account in these simulations.

Voets and coworkers recently studied random copolymers functionalized with benzene-1,3,5-tricarboxamides which were synthesized and transformed into SCNPs based on BTA self-assembly into helical aggregates as a result of strong 3-fold hydrogen bonding between the amides of adjacent BTAs.<sup>69</sup> An in depth analysis of the folding

process as a function of the chain length was obtained through the use of SANS, SAXS, and DLS. Experiments showed that there is a lack of cooperativity in the intramolecular folding of the polymer, which is unexpected because the intermolecular BTA self-assembly is typically a cooperative process.

Although studies have shown that most SCNPs mimic an intrinsically disordered globular coil, simulation of the folding transition of a single chain indicate that SCNPs have the potential to mimic the control of many natural processes. Yoshinaga et al have performed Monte Carlo simulations that provide a great comparison to SCNPs. These studies reveal the potential of SCNPs but to mimic globular proteins, but the current state of the art is far from this goal.<sup>83</sup>

A recent survey of data from the literature suggests that SCNPs do not adopt a truly compact globular conformation.<sup>84</sup> Cross-linking conditions typically involve dissolving the polymer in a good solvent, as poor solvation leads to aggregation. Consequently, cross-links are formed based on short-range interactions within a chain. The aspect ratio for an ellipsoidal structure was recently observed via SANS by Meijer et al (Fig 7a).<sup>69</sup> Similarly shaped SCNPs were also visualized via TEM in recent work from our laboratory.<sup>49</sup> Computational work by Pomposo et al (Fig 7c) suggests that using multiple different orthogonal cross-linking chemistries will induce a greater degree of collapse and lead to a more compact, globular state.<sup>72</sup> Experimentally, this has been confirmed in work from our group<sup>63</sup> and by the Meijer lab<sup>56</sup> (Fig 7b).<sup>52</sup>

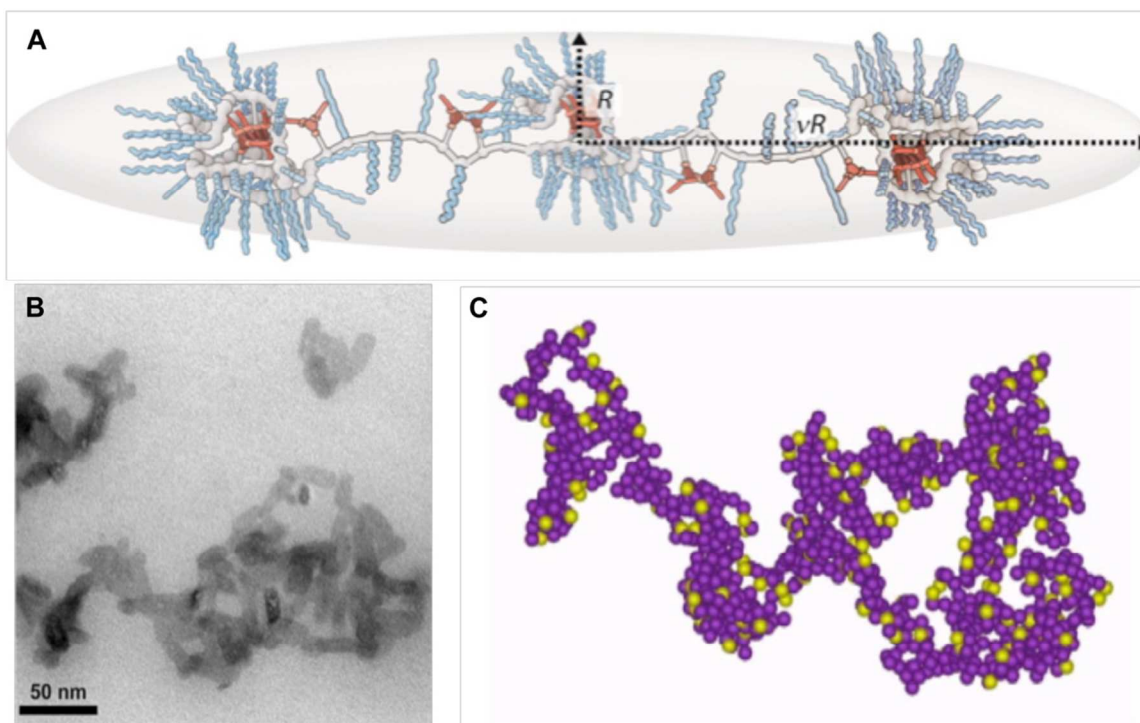


**Fig. 7** (a) Ellipsoidal structure proposed by Meijer et al; (b) visualization of ellipsoidal SCNPs formed by photocrosslinking of pendant anthracene groups; (c) SCNP structure obtained from MD simulations. Reprinted with permission from Ref. 69, 72 Copyright 2013, 2014 American Chemical Society. Reprinted with permission from Ref. 49 © 2013 WILEY-VCH Verlag GmbH & Co. KGaA, Weinheim..

**III. Potential Applications.** The potential applications of SCNPs include catalysis,<sup>1-5</sup> sensors,<sup>6</sup> nanoreactors<sup>7</sup> and nanomedicine.<sup>8-11</sup> SCNP technology is advantageous in these areas due in large part to the small size of the nanoparticles and the ease in which they can be tailored to specific uses. While the research involving SCNPs has been primarily fundamental in nature, these materials have found some practical uses. By design, the interior of the particle offers a useful chemical environment. The environment can be hydrophobic or hydrophilic, and

the size can be controlled by varying the amount of intra-chain cross-linking and the molecular weight of the parent polymer. Additionally, controlled polymerization techniques and post-polymerization modification techniques allow the incorporation of selective sites for desired function. The following section summarizes recent applied research involving SCNPs.

**Catalysis.** Enzymes are generally more efficient catalysts than their synthetic counterparts. The active site of enzymes are contained in a hydrophobic pocket, but most synthetic models are exposed to an aqueous environment.<sup>85</sup> Modeling enzymes using polymer backbones opens doors for preparing efficient catalysts by controlling properties including polymer solubility, increased accessibility to a larger library of substrates, and increased turnover frequency (TOF). Another challenge in homogenous catalysis is the regeneration of the catalyst. In most circumstances, the product and catalyst have similar solubility and the reactions are generally performed in nonaqueous solvents. This presents a disadvantage because using a homogeneous catalysts for industrial processes produces a large amount of waste during the chemical work up. Using a polymer support for catalysis is an attractive route for homogenous catalysis because the polymer and product can be easily separated.<sup>86</sup> SCNPs offer possible solutions to these challenges.

Perez-Baena et al reported a tris(pentafluorophenyl)boron ( $B(C_6F_5)_3$ ) containing SCNP.<sup>1</sup> The  $B(C_6F_5)_3$  units also serve as catalytic sites to allow the SCNP to mimic the function of reductase and polymerase. However, the enzymatic activity of the reported SCNP is limited to organic solvents such as halogenated

solvents, toluene, and benzene. Solvents that form adducts with boron are unsuitable and quench the catalytic activity. Empirical evidence demonstrates the size, composition, quantity, and location of catalytic compartments influences the kinetics and turnover frequency (TOF) of catalysis. The TOF can be improved by either decreasing the hydrodynamic radius or by increasing the molecular weight of the polymer.

Catalysis of organic reactions in water is desirable; however, many catalytic systems are compatible only with organic solvents. To address this using SCNPs, Terishima et. al. reported the synthesis of a styrene-based copolymer containing PEG, BTA, and diphenylphosphinostyrene (SDP) using ruthenium catalyzed CRP.<sup>2</sup> The copolymers were able to self-assemble and form SCNPs in an aqueous environment. The presence of SDP induced ligand exchange to incorporate the ruthenium catalyst into hydrophobic cavities within the polymer. The authors demonstrated transfer hydrogenation at the catalytic site. They found the self-assembled  $\alpha$ -helices could withstand aqueous catalytic conditions (0.4 M HCOONa and substrate at 40 °C). Cyclohexanone was efficiently reduced to cyclohexanol, and even acetophenone, which has poor water solubility, was 86% reduced after 18 h. The turnover frequency for this SCNPs based catalytic system (1-20 h<sup>-1</sup>) is comparable to other catalysts (1-40 h<sup>-1</sup>) under similar conditions.<sup>87-89</sup> In a subsequent publication from the same researchers, it was determined that the folding induced by BTA units was not essential to the catalysis; the collapse of the polymer induced by SDP ligation to ruthenium created the catalyst-containing

hydrophobic sites necessary to perform the catalysis. However, it was maintained that the SCNP-bound catalyst was more effective than the free catalyst.<sup>3</sup>

The importance of compartmentalizing an active site within a hydrophobic pocket of a polymer was shown by Huerta et al<sup>4</sup> A water soluble methacrylate copolymer was synthesized, containing self-assembling BTA units to provide a hydrophobic pocket. An L-proline analog, which is the catalytic site found in class I aldolase, was incorporated into the hydrophobic pocket of the SCNP. The catalytic activity of the nanoparticles was determined using cyclohexanone and *p*-nitrobenzaldehyde as substrates. Nearly 100% conversion to the aldol product was observed after 120 hours with the L-proline content remaining constant. Conversion was higher for polymers with higher molecular weight (~38 kDa) versus the lower molecular weight (~28 kDa), while polymers without BTA units did not demonstrate catalytic activity. The catalytic nanoparticles were also found to be re-useable. The high catalytic efficiency can be attributed to the hydrophobic environment, which brings the substrate within close proximity of the catalytic site. This leads to an increase in local concentration of the substrate near catalytic site and results in high conversion. In this case, controlling the size of the SCNP is important for tuning catalytic efficiency.

Pomposo et al reported a polymer functionalized with acetoacetoxy (AcAc) groups that formed SCNPs when introduced to copper (II) acetate. The nanoparticles were then used as a catalyst for alkyne homo-coupling. Compared to the free copper complex under the same solvent and temperature conditions, the copper (II) functionalized nanoparticle showed catalytic selectivity toward propargyl acetate and, to



a lesser extent, propargyl propionate. Also, the catalyst was effective at an overall lower catalyst concentration (0.5 mol% compared to 3 mol%).<sup>5</sup>

He and coworkers reported the synthesis of SCNPs from coumarin-containing random copolymers of poly(N,N-dimethylaminoethyl methacrylate). The SCNPs were synthesized via photo-cross-linking of the coumarin units and used as nanoreactors to synthesize gold nanoparticles (AuNP) from H<sub>2</sub>AuCl<sub>4</sub>. The authors found that a higher degree of cross-linking led to faster AuNP formation. By stirring a dilute solution of the samples with H<sub>2</sub>AuCl<sub>4</sub>, the tertiary amine units of the polymers acted as reductants and stabilizers of the gold nanoparticles. The more compact polymer provided a higher local concentration of the amine, thereby increasing the number of AuCl<sub>4</sub> ions around the nano-objects, facilitating the faster reduction. The experiment was conducted in both THF and water; AuNP formation was faster in water, since the SCNPs are less solvated and therefore more compact.<sup>7</sup>

**Nano-medicine.** Perez-Baena and coworkers developed SCNPs with multiple gadolinium (III) sites as a potential MRI contrast agent.<sup>8</sup> Azide functionalized acrylic polymers were cross-linked with the dialkyne functionalized Gd(III) diethylenetriaminepentaacetic acid (DTPA). In addition to being water soluble, the conformationally locked Gd(III) centers showed enhanced relaxation time with a 2-fold increase over a Magnevist, a commonly used MRI contrast agent, as well as a 4-fold increase over the Gd-loaded cross-linker by itself. This suggests that the SCNPs architecture was advantageous for this application.

Pomposo et al used small angle neutron scattering measurements to show their RAFT poly(MMA-*r*-AEMA) behaves like a disordered multidomain protein.<sup>9</sup> The polymer chains achieved this conformation through intra-chain Michael addition using bi- and trifunctional cross-linking units. Vitamin B<sub>9</sub> nanocarriers based on these nanoparticles demonstrated controlled release in water at neutral pH. The release of vitamin B<sub>9</sub> was monitored by UV-Vis. They observed a release exponent approximately of 0.5, which suggests the delivery process proceeds through a Fickian diffusion mechanism. The complete delivery of vitamin B<sub>9</sub> from the Michael nanoparticles with a drug loading content of 41 wt% took place in 5-6 hours.

Expanding upon their polycarbonate based nanosponges synthesized via the reaction of a diamine cross-linker with epoxide moieties,<sup>37</sup> Harth et al developed a targeted drug delivery system for breast cancer.<sup>10</sup> The researchers developed a targeting peptide capable of recognizing tumorous cells upon their exposure to ionizing radiation. The peptide was conjugated to the nanosponge via thiol-ene “click” chemistry, and the nanosponge was impregnated with the anti-cancer drug paclitaxel. Mouse studies showed that the targeted nanoparticle based system resulted in much slower tumor growth, and a greater retention of paclitaxel over time compared to systemic paclitaxel. The same researchers developed a similar system based on a lung cancer model, in which paclitaxel was administered followed by camptothecin.<sup>11</sup>

**Chemical Sensors.** Gillissen et. al. designed SCNPs that act as compartmentalized sensors for metal ions (Fig 8).<sup>6</sup> Polynorbornene polymers were cross-linked with

3,3-bis(acylamino)-2,2-bipyridine substituted benzene-1,3,5-tricarboxamides (BiPy-BTAs). The BiPy-BTA cross-linker also served as the metal binding moiety as well as the fluorescing component via aggregate induces emission. The multifunctional cross-linker is well suited for metal sensing, as the SCNPs would lose its fluorescence after binding a metal ion.

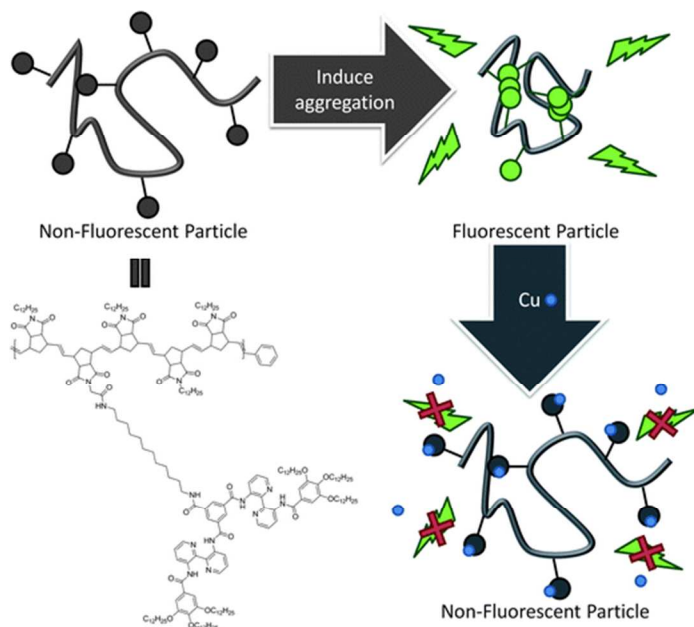


**Fig. 8** A Schematic representation of the sensing function of the BiPy-BTA functional polymers. Reproduced from Ref. 6 with permission from The Royal Society of Chemistry.

The advantage of SCNPs in this system is that the particle is inherently ratiometrically fluorescent upon formation without additional functionalization. The luminescence is caused by aggregate induced emission upon polymer folding. Subsequent quenching experiments with a variety of metals showed this system was especially sensitive to copper, which provided the most quenching.

**Self-Assembly.** In addition to the utility that SCNPs present, they may serve as building blocks for more compartmentalized nano-machinery, comparable to complex

biomacromolecules. From a primary structure inherent to the parent polymer, to secondary structures resulting through folding, it may be possible to assemble SCNPs into hierarchically ordered materials.

The secondary structures in enzymes are important for describing substructures of the macromolecule, while the tertiary structure is important for blocking or opening the active site for binding substrates. While many authors report protein-like polymers that adopt secondary structures using BTA units, very few report control over the tertiary structure. The Barner-Kowollik group has taken advantage of the orthogonal H-bonding pairs cyanuric acid-Hamilton wedge<sup>50</sup> and thymine-diaminopyridine<sup>52</sup> to mimic polymer self-folding as observed in biomolecules. In each case, one H-bonding unit was attached to an ATRP initiator. These initiators were used to synthesize polystyrene with an active bromide end group, which was used to attach the opposing H-bonding unit via “click” chemistry. In a subsequent publication, the two orthogonal pairs were combined in a single polymer; the polymer structure was designed such that each H-bonding unit was separated by a block of polystyrene.<sup>51</sup> Light scattering measurements demonstrated the reduction in hydrodynamic radius at low concentration. Variable temperature <sup>1</sup>H NMR was used to demonstrate hydrogen bonding of the cyanuric acid, Hamilton Wedge, and thymine moieties by observing changes in the NH chemical shift. This folding can be reversed upon raising the temperature of the solution to shift equilibrium towards a random coil state.

Wen et al developed self assembling monotethered SCNPs shape amphiphiles based on poly(2-(dimethylamino)ethyl methacrylate)-block-polystyrene (PDMAEMA-b-PS). The tertiary amine block was cross-linked with 1,4-diiodobutane via the

Menschutkin reaction to form “tadpole” shape amphiphiles; similar to work done by Tao and Liu,<sup>90</sup> as well as Kim et al.<sup>91</sup> These tadpole shape amphiphiles, bearing a hydrophilic SCNP head and a hydrophobic polystyrene tail, were capable of self assembling into micelles or vesicles based on solvent. The diameters of these micelles were between 30—80 nm.<sup>41</sup>

## References

1. I. Perez-Baena, F. Barroso-Bujans, U. Gasser, A. Arbe, A. J. Moreno, J. Colmenero and J. A. Pomposo, *ACS Macro Lett.*, 2013, 2, 775-779.
2. T. Terashima, T. Mes, T. F. A. De Greef, M. A. J. Gillissen, P. Besenius, A. R. A. Palmans and E. W. Meijer, *J. Am. Chem. Soc.*, 2011, 133, 4742-4745.
3. M. Artar, T. Terashima, M. Sawamoto, E. W. Meijer and A. R. A. Palmans, *Journal of Polymer Science Part A: Polymer Chemistry*, 2014, 52, 12-20.
4. E. Huerta, P. J. M. Stals, E. W. Meijer and A. R. A. Palmans, *Angew. Chem., Int. Ed.*, 2013, 52, 2906-2910.
5. A. Sanchez-Sanchez, A. Arbe, J. Colmenero and J. A. Pomposo, *ACS Macro Letters*, 2014, 3, 439-443.
6. M. A. J. Gillissen, I. K. Voets, E. W. Meijer and A. R. A. Palmans, *Polymer Chemistry*, 2012, 3, 3166-3174.
7. J. He, L. Tremblay, S. Lacelle and Y. Zhao, *Soft Matter*, 2011, 7, 2380-2386.
8. I. Perez-Baena, I. Loinaz, D. Padro, I. Garcia, H. J. Grande and I. Odriozola, *J. Mater. Chem.*, 2010, 20, 6916-6922.
9. A. Sanchez-Sanchez, S. Akbari, A. Etxeberria, A. Arbe, U. Gasser, A. J. Moreno, J. Colmenero and J. A. Pomposo, *ACS Macro Lett.*, 2013, 2, 491-495.
10. R. J. Passarella, D. E. Spratt, A. E. van der Ende, J. G. Phillips, H. Wu, V. Sathiyakumar, L. Zhou, D. E. Hallahan, E. Harth and R. Diaz, *Cancer Res.*, 2010, 70, 4550-4559.
11. G. Hariri, A. D. Edwards, T. B. Merrill, J. M. Greenbaum, A. E. van der Ende and E. Harth, *Molecular Pharmaceutics*, 2013, 11, 265-275.
12. G. Gody, T. Maschmeyer, P. B. Zetterlund and S. Perrier, *Nat Commun*, 2013, 4.
13. E. B. Berda and K. B. Wagener, in *Materials Science and Technology*, Wiley-VCH Verlag GmbH & Co. KGaA, 2006, DOI: 10.1002/9783527603978.mst0430.
14. J.-F. Lutz, M. Ouchi, D. R. Liu and M. Sawamoto, *Science*, 2013, 341.
15. M. V. Walter and M. Malkoch, *Chemical Society Reviews*, 2012, 41, 4593-4609.
16. A. W. Bosman, H. M. Janssen and E. W. Meijer, *Chemical Reviews*, 1999, 99, 1665-1688.
17. M. Ouchi, N. Badi, J.-F. Lutz and M. Sawamoto, *Nat Chem*, 2011, 3, 917-924.
18. P. Frank, A. Prasher, B. Tuten, D. Chao and E. Berda, *Appl Petrochem Res*, 2014, DOI: 10.1007/s13203-014-0046-1, 1-9.
19. B. S. Murray and D. A. Fulton, *Macromolecules (Washington, DC, U. S.)*, 2011, 44, 7242-7252.
20. M. K. Aiertza, I. Odriozola, G. Cabanero, H.-J. Grande and I. Loinaz, *Cell. Mol. Life Sci.*, 2012, 69, 337-346.
21. O. Altintas and C. Barner-Kowollik, *Macromol. Rapid Commun.*, 2012, 33, 958-971.
22. A. Sanchez-Sanchez, I. Perez-Baena and J. A. Pomposo, *Molecules*, 2013, 18, 3339-3355.
23. M. A. Gauthier, M. I. Gibson and H.-A. Klok, *Angewandte Chemie International Edition*, 2009, 48, 48-58.
24. V. A. Davankov, M. M. Ilyin, M. P. Tsyurupa, G. I. Timofeeva and L. V. Dubrovina, *Macromolecules*, 1996, 29, 8398-8403.

25. E. Harth, B. Van Horn, V. Y. Lee, D. S. Germack, C. P. Gonzales, R. D. Miller and C. J. Hawker, *J. Am. Chem. Soc.*, 2002, 124, 8653-8660.
26. A. Tuteja, M. E. Mackay, C. J. Hawker, B. Van Horn and D. L. Ho, *J. Polym. Sci., Part B: Polym. Phys.*, 2006, 44, 1930-1947.
27. J. N. Dobish, S. K. Hamilton and E. Harth, *Polymer Chemistry*, 2012, 3, 857-860.
28. T. E. Duket, M. E. Mackay, B. Van Horn, K. L. Wooley, E. Drockenmuller, M. Malkoch and C. J. Hawker, *Nano Lett.*, 2005, 5, 1704-1709.
29. J. Jiang and S. Thayumanavan, *Macromolecules*, 2005, 38, 5886-5891.
30. D. Mecerreyes, V. Lee, C. J. Hawker, J. L. Hedrick, A. Wursch, W. Volksen, T. Magbitang, E. Huang and R. D. Miller, *Adv. Mater. (Weinheim, Ger.)*, 2001, 13, 204-208.
31. O. Altintas, J. Willenbacher, K. N. R. Wuest, K. K. Oehlenschlaeger, P. Krolla-Sidenstein, H. Gliemann and C. Barner-Kowollik, *Macromolecules (Washington, DC, U. S.)*, 2013, 46, 8092-8101.
32. J. B. Beck, K. L. Killops, T. Kang, K. Sivanandan, A. Bayles, M. E. Mackay, K. L. Wooley and C. J. Hawker, *Macromolecules (Washington, DC, U. S.)*, 2009, 42, 5629-5635.
33. A. E. Cherian, F. C. Sun, S. S. Sheiko and G. W. Coates, *J. Am. Chem. Soc.*, 2007, 129, 11350-11351.
34. A. Ruiz de Luzuriaga, N. Ormategui, H. J. Grande, I. Odriozola, J. A. Pomposo and I. Loinaz, *Macromol. Rapid Commun.*, 2008, 29, 1156-1160.
35. N. Ormategui, I. Garcia, D. Padro, G. Cabanero, H. J. Grande and I. Loinaz, *Soft Matter*, 2012, 8, 734-740.
36. A. Ruiz de Luzuriaga, I. Perez-Baena, S. Montes, I. Loinaz, I. Odriozola, I. Garcia and J. A. Pomposo, *Macromol. Symp.*, 2010, 296, 303-310.
37. D. M. Stevens, S. Tempelaar, A. P. Dove and E. Harth, *ACS Macro Letters*, 2012, 1, 915-918.
38. P. T. Dirlam, H. J. Kim, K. J. Arrington, W. J. Chung, R. Sahoo, L. J. Hill, P. J. Costanzo, P. Theato, K. Char and J. Pyun, *Polym. Chem.*, 2013, 4, 3765-3773.
39. X. Jiang, H. Pu and P. Wang, *Polymer*, 2011, 52, 3597-3602.
40. A. Sanchez-Sanchez, I. Asenjo-Sanz, L. Buruaga and J. A. Pomposo, *Macromol. Rapid Commun.*, 2012, 33, 1262-1267, S1262/1261-S1262/1266.
41. J. Wen, L. Yuan, Y. Yang, L. Liu and H. Zhao, *ACS Macro Lett.*, 2013, 2, 100-106.
42. B. Zhu, G. Qian, Y. Xiao, S. Deng, M. Wang and A. Hu, *J. Polym. Sci., Part A: Polym. Chem.*, 2011, 49, 5330-5338.
43. B. Zhu, J. Ma, Z. Li, J. Hou, X. Cheng, G. Qian, P. Liu and A. Hu, *J. Mater. Chem.*, 2011, 21, 2679-2683.
44. D. E. Whitaker, C. S. Mahon and D. A. Fulton, *Angew. Chem., Int. Ed.*, 2013, 52, 956-959.
45. B. T. Tuten, D. Chao, C. K. Lyon and E. B. Berda, *Polym. Chem.*, 2012, 3, 3068-3071.
46. J.-H. Ryu, R. T. Chacko, S. Jiwanich, S. Bickerton, R. P. Babu and S. Thayumanavan, *J. Am. Chem. Soc.*, 2010, 132, 17227-17235.
47. A. Sanchez-Sanchez, D. A. Fulton and J. A. Pomposo, *Chem. Commun. (Cambridge, U. K.)*, 2014, 50, 1871-1874.

48. L. Buruaga and J. A. Pomposo, *Polymers (Basel, Switz.)*, 2011, 3, 1673-1683.
49. P. G. Frank, B. T. Tuten, A. Prasher, D. Chao and E. B. Berda, *Macromol. Rapid Commun.*, 2014, 35, 249-253.
50. O. Altintas, P. Gerstel, N. Dingenouts and C. Barner-Kowollik, *Chem. Commun. (Cambridge, U. K.)*, 2010, 46, 6291-6293.
51. O. Altintas, E. Lejeune, P. Gerstel and C. Barner-Kowollik, *Polym. Chem.*, 2012, 3, 640-651.
52. O. Altintas, T. Rudolph and C. Barner-Kowollik, *J. Polym. Sci., Part A: Polym. Chem.*, 2011, 49, 2566-2576.
53. E. J. Foster, E. B. Berda and E. W. Meijer, *Journal of the American Chemical Society*, 2009, 131, 6964-6966.
54. E. B. Berda, E. J. Foster and E. W. Meijer, *Macromolecules*, 2010, 43, 1430-1437.
55. E. J. Foster, E. B. Berda and E. W. Meijer, *Journal of Polymer Science Part A: Polymer Chemistry*, 2011, 49, 118-126.
56. N. Hosono, M. A. J. Gillissen, Y. Li, S. S. Sheiko, A. R. A. Palmans and E. W. Meijer, *Journal of the American Chemical Society*, 2012, 135, 501-510.
57. P. J. M. Stals, M. A. J. Gillissen, R. Nicolay, A. R. A. Palmans and E. W. Meijer, *Polymer Chemistry*, 2013, 4, 2584-2597.
58. T. Mes, R. van der Weegen, A. R. A. Palmans and E. W. Meijer, *Angew. Chem., Int. Ed.*, 2011, 50, 5085-5089.
59. M. Ouchi, N. Badi, J.-F. Lutz and M. Sawamoto, *Nat. Chem.*, 2011, 3, 917-924.
60. M. Seo, B. J. Beck, J. M. J. Paulusse, C. J. Hawker and S. Y. Kim, *Macromolecules (Washington, DC, U. S.)*, 2008, 41, 6413-6418.
61. S. Mavila, C. E. Diesendruck, S. Linde, L. Amir, R. Shikler and N. G. Lemcoff, *Angewandte Chemie International Edition*, 2013, 52, 5767-5770.
62. T. A. Croce, S. K. Hamilton, M. L. Chen, H. Muchalski and E. Harth, *Macromolecules*, 2007, 40, 6028-6031.
63. D. Chao, X. Jia, B. Tuten, C. Wang and E. B. Berda, *Chem. Commun. (Cambridge, U. K.)*, 2013, 49, 4178-4180.
64. C. F. Hansell, A. Lu, J. P. Patterson and R. K. O'Reilly, *Nanoscale*, 2014, 6, 4102-4107.
65. J. Willenbacher, K. N. R. Wuest, J. O. Mueller, M. Kaupp, H.-A. Wagenknecht and C. Barner-Kowollik, *ACS Macro Letters*, 2014, 3, 574-579.
66. G. Gasparini, M. Dal Molin, A. Lovato and L. J. Prins, in *Supramolecular Chemistry*, John Wiley & Sons, Ltd, 2012, DOI: 10.1002/9780470661345.smc161.
67. D. E. Whitaker, C. S. Mahon and D. A. Fulton, *Angewandte Chemie*, 2013, 52, 956-959.
68. S. Cantekin, T. F. A. de Greef and A. R. A. Palmans, *Chemical Society Reviews*, 2012, 41, 6125-6137.
69. P. J. M. Stals, M. A. J. Gillissen, T. F. E. Paffen, T. F. A. de Greef, P. Lindner, E. W. Meijer, A. R. A. Palmans and I. K. Voets, *Macromolecules*, 2014, 47, 2947-2954.
70. E. A. Appel, J. Dyson, J. del Barrio and O. A. Scherman, *Polym. Prepr. (Am. Chem. Soc., Div. Polym. Chem.)*, 2012, 53, 427.
71. E. A. Appel, J. Dyson, J. del Barrio, Z. Walsh and O. A. Scherman, *Angew. Chem., Int. Ed.*, 2012, 51, 4185-4189, S4185/4181-S4185/4111.



72. A. J. Moreno, F. Lo Verso, A. Sanchez-Sanchez, A. Arbe, J. Colmenero and J. A. Pomposo, *Macromolecules (Washington, DC, U. S.)*, 2013, 46, 9748-9759.
73. A. Anastasaki, V. Nikolaou, G. S. Pappas, Q. Zhang, C. Wan, P. Wilson, T. P. Davis, M. R. Whittaker and D. M. Haddleton, *Chemical Science*, 2014, 5, 3536-3542.
74. J. A. Pomposo, I. Perez-Baena, L. Buruaga, A. Alegria, A. J. Moreno and J. Colmenero, *Macromolecules (Washington, DC, U. S.)*, 2011, 44, 8644-8649.
75. A. Einstein, *Annalen der Physik*, 1910, 338, 1275-1298.
76. C. V. Raman, *Nature*, 1928, 121, 619.
77. P. Debye, *Journal of Applied Physics*, 1944, 15, 338-342.
78. B. H. Zimm, *The Journal of Chemical Physics*, 1945, 13, 141-145.
79. P. J. Wyatt, *Anal. Chim. Acta*, 1993, 272, 1-40.
80. E. A. Appel, J. d. Barrio, J. Dyson, L. Isaacs and O. A. Scherman, *Chem. Sci.*, 2012, 3, 2278-2281.
81. N. Hosono, M. A. J. Gillissen, Y. Li, S. S. Sheiko, A. R. A. Palmans and E. W. Meijer, *J. Am. Chem. Soc.*, 2013, 135, 501-510.
82. P. Lundberg, N. A. Lynd, Y. Zhang, X. Zeng, D. V. Krogstad, T. Paffen, M. Malkoch, A. M. Nystroem and C. J. Hawker, *Soft Matter*, 2013, 9, 82-89.
83. K. Yoshikawa and N. Yoshinaga, *J. Phys.: Condens. Matter*, 2005, 17, S2817-S2823.
84. J. A. Pomposo, I. Perez-Baena, F. Lo Verso, A. J. Moreno, A. Arbe and J. Colmenero, *ACS Macro Letters*, 2014, 3, 767-772.
85. K. H. Shaughnessy, *Chemical Reviews*, 2009, 109, 643-710.
86. C. A. McNamara, M. J. Dixon and M. Bradley, *Chemical Reviews*, 2002, 102, 3275-3300.
87. X. Li, X. Wu, W. Chen, F. E. Hancock, F. King and J. Xiao, *Organic Letters*, 2004, 6, 3321-3324.
88. X. Wu and J. Xiao, *Chemical Communications*, 2007, DOI: 10.1039/B618340A, 2449-2466.
89. J. Liu, Y. Zhou, Y. Wu, X. Li and A. S. C. Chan, *Tetrahedron: Asymmetry*, 2008, 19, 832-837.
90. J. Tao and G. Liu, *Macromolecules*, 1997, 30, 2408-2411.
91. Y. Kim, J. Pyun, J. M. J. Fréchet, C. J. Hawker and C. W. Frank, *Langmuir*, 2005, 21, 10444-10458.